Cu(II) coordination polymers as vehicles in the A^3 coupling

Article (Accepted Version)

Cu(II) coordination polymers as vehicles in the A^3 coupling

Edward Loukopoulos,[a] *Michael Kallitsakis,*[a,b] *Nikolaos Tsoureas,*[a] *Alaa Abdul-Sada,*[a] *Nicholas F. Chilton,*[c] *Ioannis N. Lykakis*[*b] *and George E. Kostakis*[*a]

[a]Department of Chemistry, School of Life Sciences, University of Sussex, Brighton BN1 9QJ, United Kingdom.

E-mail: G.Kostakis@sussex.ac.uk

[b]Department of Chemistry, Aristotle University of Thessaloniki, Thessaloniki 54124, Greece.

E-mail: lykakis@chem.auth.gr

[c]School of Chemistry, The University of Manchester, Manchester M13 9PL, United Kingdom.

ABSTRACT

A family of benzotriazole based coordination compounds, obtained in two steps and good yields from commercially available materials, formulated $[Cu^{II}(L^1)_2(MeCN)_2]\cdot 2(ClO_4)\cdot MeCN$ (**1**), $[Cu^{II}(L^1)(NO_3)_2]\cdot MeCN$ (**2**), $[Zn^{II}(L^1)_2(H_2O)_2]\cdot 2(ClO_4)\cdot 2MeCN$ (**3**), $[Cu^{II}(L^1)_2Cl_2]_2$ (**4**), $[Cu^{II}_5(L^1)_2Cl_{10}]$ (**5**), $[Cu^{II}_2(L^1)_4Br_2]\cdot 4MeCN\cdot(Cu^{II}_2Br_6)$ (**6**), $[Cu^{II}(L^1)_2(MeCN)_2]\cdot 2(BF_4)$ (**7**), $[Cu^{II}(L^1)_2(CF_3SO_3)_2]$ (**8**), $[Zn^{II}(L^1)_2(MeCN)_2]\cdot 2(CF_3SO_3)$ (**9**), $[Cu^{II}_2(L^2)_4(H_2O)_2]\cdot 4(CF_3SO_3)\cdot 4Me_2CO$ (**10**) and $[Cu^{II}_2(L^3)_4(CF_3SO_3)_2]\cdot 2(CF_3SO_3)\cdot Me_2CO$ (**11**) are reported. These air stable compounds were tested as homogeneous catalysts for the A^3 coupling synthesis of propargyl amine derivatives from aldehyde, amine and alkyne under a non-inert atmosphere. Fine-tuning of the catalyst resulted in a one dimensional (1D) coordination polymer (CP) (**8**) with excellent catalytic activity in a wide range of substrates, avoiding any issues that would inhibit its performance.

Introduction

Coordination polymers (CPs) are compounds constructed from metal centers and polytopic organic ligands through coordination bonds, in order to form structures that extend into one, two or three dimensions.[1] These species have received tremendous attention due to their use in gas sorption,[2] drug delivery,[3,4] luminescence,[5] magnetism,[6] sensing[7] and catalysis[8]. The latter application has been thoroughly studied for porous three dimensional CPs, also known as metal organic frameworks (MOFs); however, there is a significant impact on their preparation and handling[9]. One dimensional (1D) CPs are typically easy to synthesize and their composition may be easily tuned, *via* variation of ligand/metal/counter ion, in order to optimize their application potential,[10–12] of which most interestingly, their catalytic properties have been scarcely studied.[13–18]

The metal catalyzed multi-component reaction (MCR) of an aldehyde, an amine and an alkyne, also known as the A^3 coupling, has gathered significant interest.[19–27] This coupling reaction yields propargyl amines, which have been proposed as key intermediates in the synthesis of nitrogen-containing biologically active compounds such as acrylamidines,[28] oxazoles,[29,30] pyrroles,[31] pyrrolidines[32] as well as natural products.[33,34] Due to this importance, a large variety of metal sources have been employed to catalyze this reaction such as Au(I)/Au(III),[35–37] Ag(I),[38–41] Cu(I),[26,42–45] In(III)[46] or Rh(III).[47] More common transition metals, such as Cu(II),[48–50] Fe(III),[51–53] Ni(II)[54] and Zn(II)[55] have also been occasionally employed, albeit with higher catalyst loadings and under inert conditions.

Benzotriazole has been extensively used in organic transformations as auxiliary[56] or to yield other heterocycles[57]. More importantly in the context of this work, its derivatives provide enormous coordination versatility in combination with transition metal ions,[58] to yield coordination polymers[59–63] or coordination clusters.[64,65] Our previous studies focused on the catalytic potential of one- and two-dimensional CPs[66] and were focused in semi-rigid

benzotriazole-based ligands.[67,68] As the organic ligand 1,2-bis((1H-benzo[d][1,2,3]triazol-1-yl)methyl)benzene (**L^1**, Scheme 1) has not been extensively used in coordination chemistry, we recently used it to synthesize three 1D CPs, formulated as $[Cu^{II}(L^1)_2(MeCN)_2]\cdot 2(ClO_4)\cdot MeCN$ (**1**), $[Cu^{II}(L^1)(NO_3)_2]\cdot MeCN$ (**2**), and $[Zn^{II}(L^1)_2(H_2O)_2]\cdot 2(ClO_4)\cdot 2MeCN$ (**3**).[69] Astonishingly, only **1** was found to catalyse the one pot synthesis of N-substituted dihydropyridines, from azines and ethyl propiolate,[69] whereas **2** and **3** were catalytically inactive. This big discrepancy in catalytic activity can be explained by the different coordination environment (**1** and **2**) as well as metal center (**1** and **3**). Moreover, the catalytic performance of **1** is inhibited due to its conversion to the catalytic inactive $[Cu^{I}(L^1)Cl]$ (**1'**) specie (ClO_4^- is converted to Cl^-), confirmed by single crystal X-ray analysis.

Encouraged from our recent study, we decided on further exploring the coordination capabilities of L^1 and its derivatives L^2 and L^3 with other Cu salts to characterize new coordination polymers and use them as catalysts towards chemical transformations of current high interest. The ultimate goal of this research is to establish a library of 1D coordination polymers as catalysts and by fine tuning their composition to be able to optimize their catalytic performance as well as to gain useful mechanistic insights. To the best of our knowledge, 1D Cu(II) CPs have not been employed as catalysts for the A^3 coupling so far. Therefore, we report the synthesis and characterization of eight new compounds formulated as $[Cu^{II}(L^1)_2Cl_2]_2$ (**4**), $[Cu^{II}_5(L^1)_2Cl_{10}]$ (**5**), $[Cu^{II}_2(L^1)_4Br_2]\cdot 4MeCN\cdot(Cu^{II}_2Br_6)$ (**6**), $[Cu^{II}(L^1)_2(MeCN)_2]\cdot 2(BF_4)$ (**7**), $[Cu^{II}(L^1)_2(CF_3SO_3)_2]$ (**8**), $[Zn^{II}(L^1)_2(MeCN)_2]\cdot 2(CF_3SO_3)$ (**9**) $[Cu^{II}_2(L^2)_4(H_2O)_2]\cdot 4(CF_3SO_3)\cdot 4Me_2CO$ (**10**) and $[Cu^{II}_2(L^3)_4(CF_3SO_3)_2]\cdot 2(CF_3SO_3)\cdot Me_2CO$ (**11**), as well as the catalytic application of **1** – **11** in to the A^3 coupling reaction between aldehydes, alkynes and amines yielding the corresponding propargylamines derivatives.

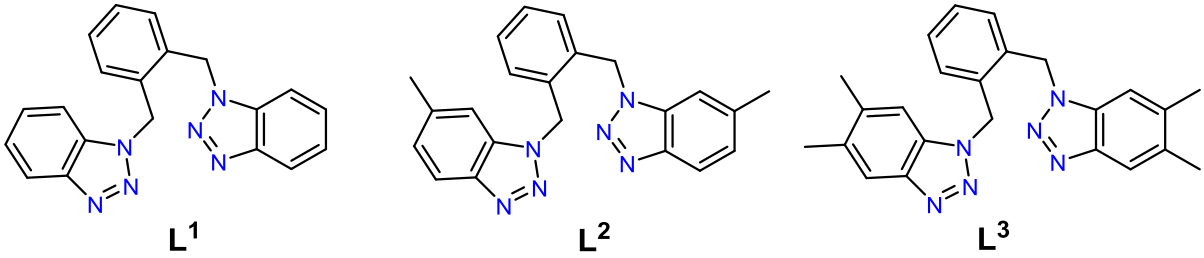

Scheme 1. The organic ligands (**L^1-L^3**) used in this study.

EXPERIMENTAL

Materials. Chemicals (reagent grade) were purchased from Sigma Aldrich, Acros Organics and Alfa Aesar. Materials and solvents were used with no further purification. Ligand L^1 and compounds **1-3** were synthesized according to the reported procedure[69]. *Safety note*: Perchlorate salts are potentially explosive; such compounds should be used in small quantities and handled with caution and utmost care at all times.

Instrumentation. IR spectra of the samples were recorded over the range of 4000-650 cm^{-1} on a Perkin Elmer Spectrum One FT-IR spectrometer fitted with a UATR polarization accessory. EI-MS was performed on a VG Autospec Fissions instrument (EI at 70 eV). TGA analysis was performed on a TA Instruments Q-50 model (TA, Surrey, UK) under nitrogen and at a scan rate of 10°C/min. NMR spectra were measured on a Varian VNMRS solution-state spectrometer at 30°C. Chemical shifts are quoted in parts per million (ppm). Coupling constants (J) are recorded in Hertz (Hz). UV-Vis measurements were performed on a Thermo Scientific Evolution300 UV-Vis Spectrophotometer and the collected data were processed using the Vision Pro software. Cyclic voltammetry studies were performed using a BASi-Epsilon potentiostat under computer control. IR drop was compensated using the feedback method. Cyclic voltammetry experiments were performed using a three-electrode configuration with glassy carbon disc (7.0 mm^2) as the working electrode, a Pt wire as the counter electrode and Ag wire as the pseudoreference electrode. Sample solutions were prepared by dissolving the

analyte (ca. 5 mM) in DMSO (1 ml) followed by addition of 0.05 M of the supporting electrolyte [$^{n}Bu_4N$][PF_6]. The reported half potentials are referenced to the $FeCp_2^{+/0}$ redox couple, which was measured by adding ferrocene (ca. 1 mg) to the sample solution. Magnetic measurements were performed on crushed crystalline samples using a Quantum Design MPMS XL7 SQUID magnetometer.

X-Ray crystallography. Data for compounds **4**, **5** and **9** were collected (ω-scans) at the University of Sussex using an Agilent Xcalibur Eos Gemini Ultra diffractometer with CCD plate detector under a flow of nitrogen gas at 173(2) K and Cu Kα radiation (λ = 1.54184 Å). CRYSALIS CCD and RED software was used respectively for data collection and processing. Reflection intensities were corrected for absorption by the multi-scan method. Data for **6**-**8** and **10** were collected at the National Crystallography Service, University of Southampton.[70] All structures were determined using Olex2[71], solved using SHELXT[72,73] and refined with SHELXL-2014[74]. All non-H atoms were refined with anisotropic thermal parameters, and H-atoms were introduced at calculated positions and allowed to ride on their carrier atoms. Compound **9** is isostructural to **8** (unit cell comparison, ESI) and its formula was confirmed by ESI-MS, TGA and CHN analysis, however the lattice OTf molecules were not possible to be refined with anisotropic parameters, therefore the SQUEEZE method was applied to remove them. For compound **11**, three different crystallographic datasets (University of Sussex, National Crystallography Service, University of Southampton, Diamond Source) confirmed the synthesis of the proposed formula, also suggested from ESI-MS, TGA and CHN analysis (see ESI). However, despite producing large block shaped green crystals, none of these datasets fulfilled the publication criteria, therefore the cif file is not provided; a figure of the structure showing connectivity is provided in the ESI. Crystal data and structure refinement parameters for newly reported compounds are given in Tables S1-S2. Geometric/crystallographic calculations were performed using PLATON[75], Olex2[71], and WINGX[74] packages; graphics

were prepared with Crystal Maker and MERCURY[76]. Each of the crystal structures (**4**-**10**) has been deposited at the CCDC 1522927-1522931, 1538190 and 1538191.

SYNTHETIC PROCEDURES

General Catalytic Protocol for A^3 coupling. A mixture of aldehyde (1 mmol), amine (1.1 mmol), alkyne (1.2 mmol), Cu catalyst (2 mol%, based on aldehyde amount) and 2-propanol (5 ml) was added into a sealed tube and stirred at 90 °C for selected time. The reaction was monitored by thin layer chromatography (TLC). After completion, the slurry was filtered upon a short pad of silica (to withhold the catalyst) and the filtrate was evaporated under vacuum. The resulting residue was then loaded to a flash column chromatography and the product propargyl amine was isolated through a silica gel using a mixture of hexane/EtOAc in a ratio of 10/1, as the eluent.

Synthesis of 1-(2-((5-methyl-1H-benzo[d][1,2,3]triazol-1-yl)methyl)benzyl)-5-methyl-1H-benzo[d][1,2,3]triazole (**L^2**). 5-methyl-1H-benzotriazole (2.796 g, 21.0 mmol) was dissolved in acetone (40 mL) and then potassium carbonate (6 g, 43 mmol) and potassium iodide (0.50 g, 3.01 mmol) were added. After stirring for 30 min, solid α,α'-dichloro-o-xylene (1.75 g, 10.0 mmol) was added slowly. The mixture was refluxed for 5 hrs. After cooling, the solution was filtered and the filtrate was evaporated to dryness. The resulting colourless syrup was then dissolved in 20 ml methanol after which a white microcrystalline precipitate was formed. Yield: 33% (1.2 g). Selected IR peaks (cm^{-1}): 2972 (w), 1624 (w), 1501 (m), 1455 (m), 1311 (w), 1278 (m), 1265 (w), 1222 (s), 1163 (w), 1135 (w), 1117 (m), 1103 (m), 1075 (m), 1039 (w), 951 (m), 930 (m), 860 (m), 801 (s), 757 (s), 740 (s), 722 (s), 693 (m), 664 (w), 616 (m). HRMS for $C_{22}H_{21}N_6$ [M + H]: theor. 369.1827 m/z, calcd. 369.1822 m/z.

Synthesis of 1-(2-((5,6-dimethyl-1H-benzo[d][1,2,3]triazol-1-yl)methyl)benzyl)-5,6-dimethyl-1H-benzo[d][1,2,3]triazole (**L^3**). 5,6-Dimethyl-1H-benzotriazole monohydrate (1.3

g, 8 mmol) was dissolved in acetone (30 mL) and then potassium carbonate (2.2 g, 16 mmol) and potassium iodide (0.50 g, 3.01 mmol) were added. After stirring for 30 min, solid α,α'-dichloro-o-xylene (0.65 g, 3.75 mmol) was added slowly. The mixture was refluxed for 5 hrs. After cooling, the solution was filtered and the filtrate was evaporated to dryness after which a brown microcrystalline precipitate was formed. Yield: 93% (1.38 g). Selected IR peaks (cm^{-1}): 2974 (w), 1630 (w), 1493 (m), 1449 (m), 1372 (w), 1314 (w), 1284 (m), 1259 (w), 1222 (s), 1158 (w), 1117 (m), 1102 (m), 1070 (m), 1049 (w), 1023 (w), 999 (m), 934 (m), 846 (s), 784 (w), 746 (s), 718 (s), 685 (m), 664 (w), 606 (m). HRMS for $C_{24}H_{25}N_6$ [M + H]: theor. 397.2140 m/z, calcd. 397.2135 m/z.

Synthesis of $[Cu^{II}(L^1)Cl_2]_2$ (**4**). 0.12 mmol (0.041 g) of L and 0.12 mmol (0.016 g) of anhydrous $CuCl_2$ were dissolved in 8 ml MeCN while stirring to produce a yellow solution. After a further 15 minutes of stirring, the solution was filtrated, stored in a glass vessel and heated at 75 °C for 18 hours to produce large green block crystals. Selected IR peaks (cm^{-1}): 1590 (w), 1492 (w), 1455 (m), 1315 (m), 1290 (w), 1235 (w), 1145 (w), 1015 (w), 1006 (w), 952 (m), 900 (w), 778 (m), 770 (m), 729 (s), 661 (m). Yield: 18% (based on Cu). Elemental analysis for $C_{40}H_{32}Cl_4Cu_2N_{12}$: calcd. C 50.74, H 3.41, N 17.76; found C 50.79, H 3.46, N 17.89.

Synthesis of $[Cu^{II}_5(L^1)_2Cl_{10}]$ (**5**). 0.12 mmol (0.041 g) of L and 0.36 mmol (0.048 g) of anhydrous $CuCl_2$ were dissolved in 8 ml MeCN while stirring to produce a yellow solution. After a further 15 minutes of stirring, the solution was filtrated, stored in a glass vessel and heated at 95 °C for 18 hours to produce good quality brown block crystals. Selected IR peaks (cm^{-1}): 1589 (w), 1492 (w), 1452 (m), 1370 (w), 1331 (m), 1313 (w), 1278 (w), 1231 (m), 1165 (w), 1144 (w), 1002 (w), 970 (w), 961 (w), 841(w), 792 (w), 779 (w), 752 (m), 738 (s), 711 (m), 668 (m). Yield: 33% (based on Cu). Elemental analysis for $C_{40}H_{32}Cl_{10}Cu_5N_{12}$: calcd. C 35.70, H 2.40, N 12.50; found C 35.59, H 2.46, N 12.43.

Synthesis of $[Cu^{II}_2(L^1)_4Br_2]\cdot 4MeCN\cdot(Cu^{II}_2Br_6)$ (**6**). Anhydrous $CuBr_2$ was used as the metal salt in a procedure similar to the synthesis of **4**. The resultant dark green solution was stored in a vial at room temperature. Small green crystals were obtained after 3 days. Selected IR peaks (cm^{-1}): 1594 (w), 1494 (s), 1456 (m), 1321 (w), 1283 (w), 1233 (m), 1167 (m), 1144 (m), 1002 (w), 966 (w), 843 (w), 789 (m), 736 (s), 670 (w), 628 (m). Yield: 11% (based on Cu). Elemental analysis for $C_{88}H_{76}Br_8Cu_4N_{28}$: theor. C 43.69, H 3.17, N 16.21; found C 43.81, H 3.13, N 16.11.

Synthesis of $[Cu^{II}(L^1)_2(MeCN)_2]\cdot 2(BF_4)$ (**7**). 0.24 mmol (0.082 g) of L were dissolved in 10 ml MeCN while stirring to produce a colourless solution. A solution containing 0.48 mmol (0.170 g) of $Cu(BF_4)_2\cdot 6H_2O$ in MeCN (7.5 ml) was slowly added. The resulting green solution was filtrated and kept stored at room temperature. Green block crystals were obtained after 1 day. Selected IR peaks (cm^{-1}): 3468 (w), 3508 (w), 1651 (w), 1592 (w), 1495 (w), 1454 (m), 1320 (m), 1282 (m), 1234 (m), 1172 (m), 1159 (w), 1060 (s), 1017 (s), 969 (m), 953 (w), 853 (w), 793 (w), 780 (m), 757 (s), 748 (s), 739 (s), 672 (w). Yield: 49% (based on Cu). Elemental analysis for $C_{44}H_{38}B_2CuF_8N_{14}$: theor. C 52.84, H 3.83, N 19.62; found C 52.92, H 3.86, N 19.70.

Synthesis of $[Cu^{II}(L^1)_2(CF_3SO_3)_2]$ (**8**). 0.24 mmol (0.082 g) of L and 0.48 mmol (0.180 g) of $Cu(OTf)_2\cdot H_2O$ were dissolved in 15 ml Me_2CO while stirring to produce a dark green solution. After stirring for 1 hr, the solution was filtrated, then layered over n-hexane in a 1:2 ratio to produce large blue block crystals after 7 days. Selected IR peaks (cm^{-1}): 1589 (w), 1492 (w), 1457 (m), 1320 (m), 1275 (m), 1244 (m), 1163 (w), 1140 (m), 1023 (s), 952 (w), 848 (w), 779 (m), 746 (s), 669 (m). Yield: 11% (based on Cu). Elemental analysis for $C_{42}H_{32}CuF_6N_{12}O_6S_2$: calcd. C 48.41, H 3.10, N 16.14; found C 48.53, H 3.04, N 16.07.

Synthesis of $[Zn^{II}(L^1)_2(MeCN)_2]\cdot 2(CF_3SO_3)$ (**9**). 0.24 mmol (0.082 g) of L^1 were dissolved in 15 ml MeCN while stirring to produce a colorless solution. 0.12 mmol (0.044 g) of $Zn(OTf)_2$ were then added. After stirring for a further 30 min., the resulting colorless solution was

filtrated, then layered over Et_2O in a 1:2 ratio. Large colorless block crystals were obtained after 2 weeks. Selected IR peaks (cm^{-1}): 3434 (br), 1654(w), 1592 (w), 1494 (w), 1456 (m), 1372 (w), 1319 (m), 1269 (m), 1226 (s), 1153 (m), 1094 (w), 1025 (s), 951 (w), 880 (w), 843 (w), 766 (w), 740 (s), 714 (w), 669 (m). Yield: 38% (based on Zn). Elemental analysis for $C_{46}H_{38}F_6N_{14}O_6S_2Zn$: C 49.04, H 3.40, N 17.42; found C 49.11, H 3.53, N 17.38.

Synthesis of $[Cu^{II}_2(L^2)_4(H_2O)_2]\cdot 4(CF_3SO_3)\cdot 4Me_2CO$ (**10**). 0.1 mmol (0.036 g) of L^2 and 0.1 mmol (0.037 g) of $Cu(OTf)_2\cdot H_2O$ were dissolved in 15 ml acetone while stirring to produce a turquoise solution. The solution was filtrated, then layered over n-hexane in a 1:2 ratio to produce green needle-like crystals after a few hours. Selected IR peaks (cm^{-1}): 1592 (w), 1504 (w), 1457 (m), 1279 (m), 1223 (s), 1158 (m), 1027 (s), 868 (w), 805 (m), 758 (w), 721 (w), 636 (s). Yield: 23% (based on Cu). Elemental analysis for $C_{104}H_{108}Cu_2F_{12}N_{24}O_{18}S_4$: C 50.65, H 4.42, N 13.64; found C 50.73, H 4.36, N 13.63.

Synthesis of $[Cu^{II}_2(L^3)_4(CF_3SO_3)_2]\cdot 2(CF_3SO_3)\cdot Me_2CO$ (**11**). 0.12 mmol (0.048 g) of L^3 and 0.24 mmol (0.089 g) of $Cu(OTf)_2\cdot H_2O$ were dissolved in 15 ml acetone while stirring to produce a dark green solution. The solution was filtrated, then layered over n-hexane in a 1:2 ratio to produce small green block crystals after 10 days. Selected IR peaks (cm^{-1}): 3436 (br), 1707 (w), 1631 (w), 1590 (w), 1559 (w), 1494 (w), 1456 (m), 1252 (m), 1235 (s), 1221 (s), 1153 (m), 1026 (s), 1003 (m), 965 (w), 901 (w), 845 (m), 785 (w), 748 (m). Yield: 10% (based on Cu). Elemental analysis for $C_{103}H_{102}Cu_2F_{12}N_{24}O_{13}S_4$: C 52.25, H 4.35, N 14.21; found C 52.33, H 4.41, N 14.34.

RESULTS

Synthetic aspects. A crystalline material was obtained through a variety of techniques: leaving the sample undisturbed in room temperature (**1**, **3**, **6**, **7**), solvothermal conditions (**4**, **5**) or liquid diffusion (**2**, **8** – **11**). All reactions, with the exception of compounds **4** and **5**, are not sensitive

to the Cu(II):L molar ratio; ratios from 3:1 to 1:3 yield the same compound in comparable yields and purity. In the case of **4** and **5**, the final product depends on the appropriate ratio of starting materials (1:1 and 3:1, respectively) and temperature (75° and 95°C, respectively). The metal centre (Cu(II) or Zn(II)) is not coordinated to the N2 nitrogen atom of the benzotriazole molecules in any of the compounds; this may be attributed to the steric effects of the bulky CH_2-C_6H_4-CH_2 unit. All compounds are soluble in DMF and slightly soluble in other common organic solvents (e.g. acetonitrile, methanol, THF); their solubility in these solvents increases greatly when heated. However, they are insoluble in water.

Crystal structure description. The crystal structures of **1** – **3** were recently reported, however they will be described in detail to facilitate discussion and comparison with compounds **4** – **11**. Compound **1** crystallizes in the triclinic space group $P\bar{1}$ and contains one molecule in the asymmetric unit. The unit consists of a Cu(II) center, one organic ligand molecule, a perchlorate lattice anion, and two acetonitrile solvent molecules, out of which one acts as a terminal ligand and one is in the lattice; the latter will not be further discussed. In this conformation of the ligand (Table 1, Mode A), the angle between the planes of the benzotriazole molecules is 123.00(5)°. As a result, the structure extends to one dimension along the *a* axis, forming a 1D framework with small voids (Figure 1). Cu(II) is coordinated to six nitrogen atoms and possesses a distorted octahedral geometry, in which the axial positions are occupied by the acetonitrile nitrogen atoms. The relevant N - Cu - N bond angles range from 87.02(7)° to 92.98(7)°. As for the relevant bond lengths, the mean Cu-N_{ligand} distances are 2.0815(16) and 2.0133(17) Å, significantly shorter than the respective Cu-$N_{acetonitrile}$ distance which was measured at 2.422(2) Å. No strong hydrogen bonds or other supramolecular interactions are observed. Additionally, compounds **3**, **7** and **9** were found to be isostructural to **1**; In **7**, (Figure S3, ESI) the counter anion is BF_4^- instead of ClO_4^-. **3** was synthesized using $Zn(ClO_4)_2 \cdot 6H_2O$ and shows an identical 1D framework, however the two coordinating

acetonitrile moieties are replaced by H_2O molecules (Figure S2, ESI). **9** is another Zn(II) compound that is a similar 1D CP and contains $CF_3SO_3^-$ anions in the lattice (Figure S4, ESI). As a result, these structures will not be further described.

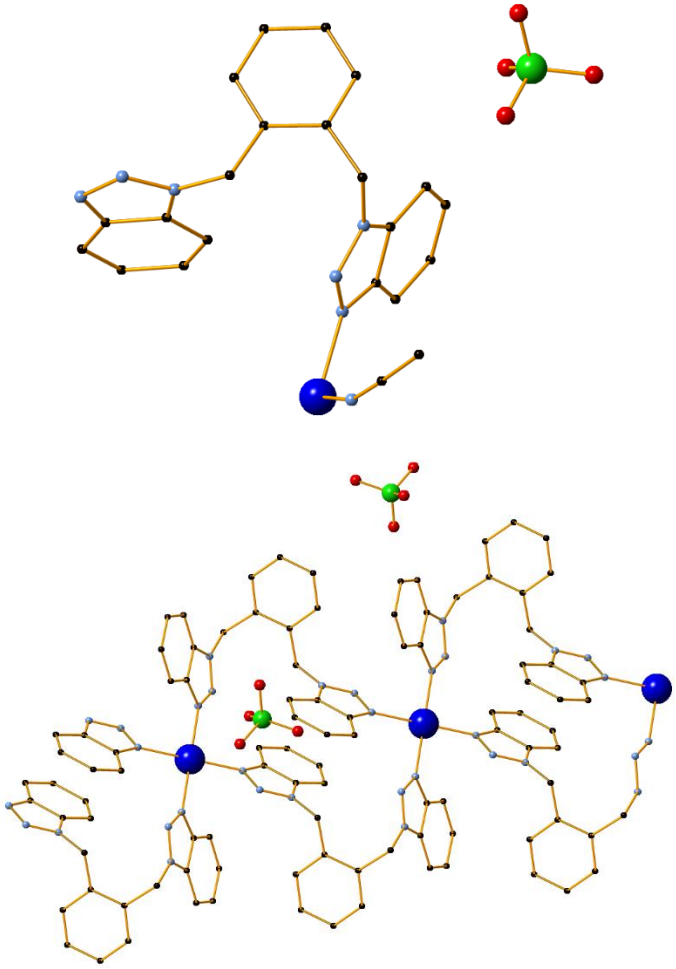

Figure 1. (upper) The asymmetric unit of **1**. H atoms are omitted for clarity. (lower) Part of the one-dimensional framework of **1**. H atoms, certain perchlorate anions and solvent molecules are omitted for clarity. Color code Cu (blue), C (black), N (light blue), Cl (green), O (red).

In compound **2** the complex crystallizes in the monoclinic $P2_1/n$ space group. Its asymmetric unit consists of a Cu(II) center, one organic ligand molecule, two nitrate anions and one acetonitrile solvent molecule (Figure S1, ESI). The coordination mode of the ligand is the same to the mode in **1** (Table 1, Mode A). The presence of the chelating and bridging nitrate moieties leads to the formation of an unusual dimeric Cu_2 unit as the structure extends in two

dimensions along the *b0c* plane (Figure 2). A search in the Cambridge Structure Database[77] reveals no other example of Cu_2 unit based on nitrates. The metal center has a coordination environment of $\{N_2O_5\}$ and possesses a pseudo-octahedral geometry; five nitrate oxygen atoms occupy the equatorial positions of the pseudo-octahedron, while two nitrogen atoms from ligand molecules occupy the axial positions. The mean Cu-N distances are 1.9849(6) and 1.9916(6) Å, while the Cu-O distances range from 1.9813(6) to 2.6587(6) Å. The relevant N-Cu-O bond angles range from 85.32(4)° to 95.66(4)°.

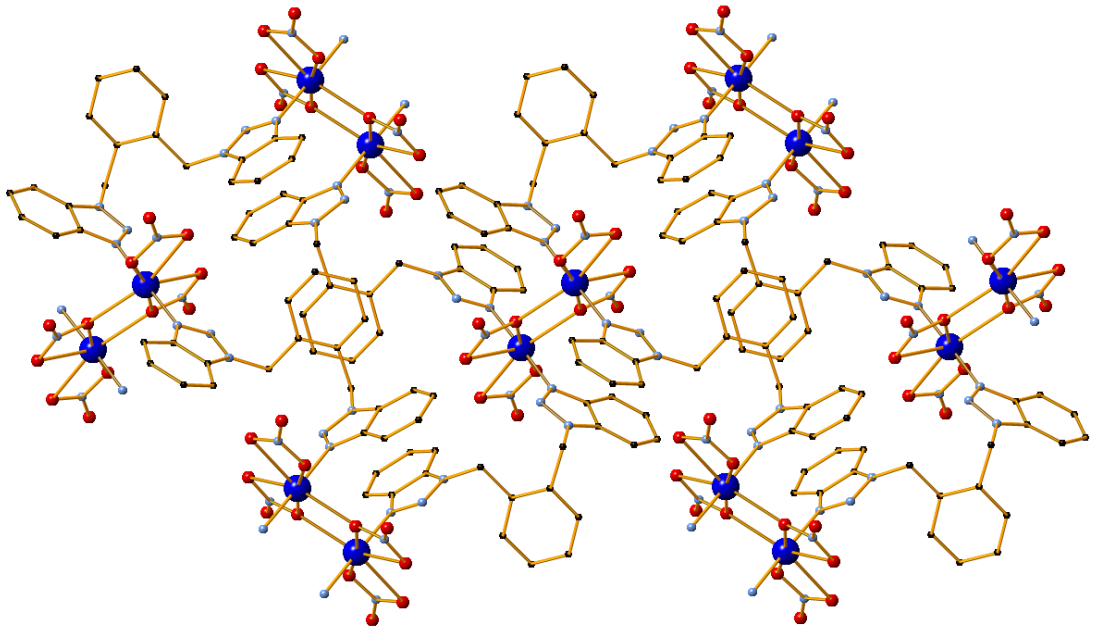

Figure 2. Part of the two-dimensional framework of **2**. H atoms are omitted for clarity. Color code Cu (blue), C (black), N (light blue), O (red).

Compound **4** crystallizes in the triclinic $P\bar{1}$ space group and consists of two $[Cu_2L_2Cl_4]$ units. All metal centers in the structure show a distorted trigonal bipyramidal geometry through a coordination environment of $\{N_2Cl_3\}$ (τ = 0.46 for Cu1, 0.40 for Cu2)[78]. The basal plane in the geometries of both metal centers consists of chloride atoms, while ligand nitrogen atoms are in the axial positions. These units are not further linked through intermolecular interactions and each ligand adopts a syn-conformation regarding the position of the benzotriazole groups

(Table 1, Mode B). This accounts for the eventual formation of zero-dimensional dimeric units (Figure 3, upper). The mean Cu-N distances are 2.015(4) and 2.028(4) Å. Cl-Cu-Cl bond angles range from 93.65(4)° to 154.33(6)° while the respective values for the N-Cu-N angles are 177.47(17)° and 178.44(17)°.

Compound **5** also crystallizes in the triclinic $P\bar{1}$ space group. However, in this case the asymmetric unit contains two full-occupancy and one half-occupancy Cu(II) centers, as well as one ligand molecule and five chlorine atoms. Two of the metal centers (Cu2, Cu3) are coordinated to the ligand and to chlorine atoms, while the third (Cu1) is only coordinated to chlorine atoms and bridges the $[Cu_2L_2]$ nodes. The ligand adopts the same conformation as in Mode A, but a different coordination mode (Table 1, Mode C). All of the above lead to the formation of an unusual two-dimensional coordination polymer which extends along the *a0c* plane, as shown in Figure 3 (lower). The coordination environment and geometries of the metal centers are also varied. Cu1 is coordinated to five chlorine atoms and exhibits a distorted square pyramidal geometry ($\tau = 0.15$)[78]. The basal plane in this geometry has a mean deviation of 0.129 Å. Cu2 is also coordinated to five atoms and possesses a distorted square pyramidal geometry ($\tau = 0.09$)[78], however in this case the basal plane consists of three chlorine atoms and one ligand nitrogen atom, while the axial position is occupied by another ligand nitrogen atom, resulting in a $\{N_2Cl_3\}$ coordination environment. In this case, the respective plane has a deviation of 0.151 Å. Finally, Cu3 shows a $\{N_2Cl_4\}$ coordination environment; consistent with an octahedral geometry, in which the ligand nitrogen atoms occupy the axial positions while chlorine atoms form the basal plane. The mean Cu-Cl bond distances range from 2.2671(12) to 2.6348(10) Å, while the respective Cu-N bond lengths range from 2.016(3) to 2.425(3) Å.

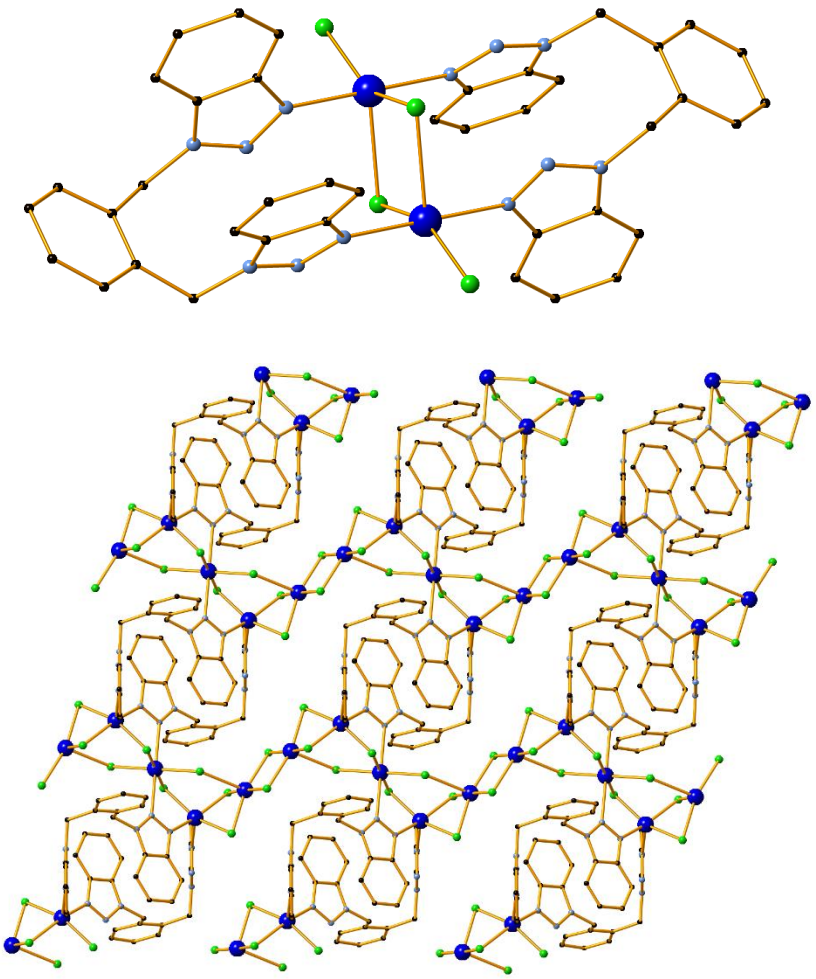

Figure 3. The structures of compounds **4** (zero-dimensional dimer, upper) and **5** (two-dimensional framework, lower). H atoms are omitted for clarity. Color code Cu (blue), C (black), N (light blue), Cl (green).

Compound **6** was synthesized using $CuBr_2$ and crystallizes in the monoclinic C2/c space group. The main core of the structure consists of a $[Cu_2L_4Br_2]^{2+}$ dicationic dimer. A dianionic $[Cu_2Br_6]^{2-}$ unit is also present and completes the charge balance for all Cu(II) centers. In similar fashion to **4**, this dimer does not form any intermolecular interactions and thus the structure is zero-dimensional **(**Figure 4). In this case the angle between the planes of the benzotriazole molecules of the ligand was measured at 125.4(4)°, similar to the one in Mode A. However, a concurrent rotation of the non-rigid C-N bond is also observed, leading to a

different conformation mode (Table 1, Mode D). The metal center that shows ligand coordination (Cu1) possesses a distorted trigonal bipyramidal ($\tau = 0.65$)[78] geometry through a $\{N_4Br\}$ environment. The bromine atom and two nitrogen atoms from ligand molecules consist of the basal plane, with the relevant angles ranging from 102.2(5)° to 139.0(3)°. The two remaining nitrogen atoms also derive from ligand molecules and occupy the axial positions of the bipyramid.

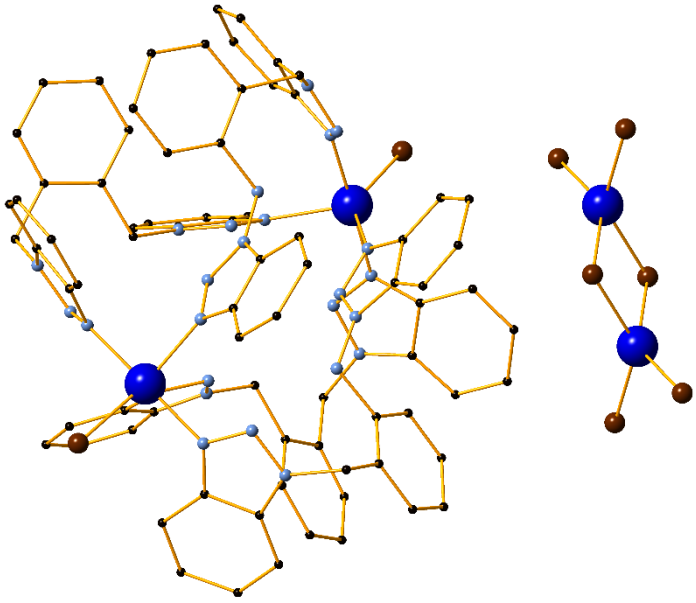

Figure 4. The structure of compound **6**. H atoms and solvent molecules are omitted for clarity. Color code Cu (blue), C (black), N (light blue), Br (brown).

Compound **8** crystallizes in the triclinic $P\bar{1}$ space group and its asymmetric unit contains a Cu(II) centre, one organic ligand molecule and one triflate anion molecule. The metal centre is coordinated to a total of six atoms and possesses an octahedral geometry through a $\{N_4O_2\}$ coordination environment. The complex shows an identical one-dimensional framework to the one of compounds **1**, **3**, **7** and **9**; the only difference is that the axial positions of the octahedron are now occupied by triflate oxygen atoms instead of acetonitrile nitrogen (Figure 5). Consequently, the ligand adopts the same coordination mode as in the aforementioned

compounds (Mode A). The mean Cu-O distance was measured at 2.536(4) Å, while the Cu-N bond lengths are 2.009(5) and 2.013(7) Å. No strong hydrogen bonds or other supramolecular interactions are observed.

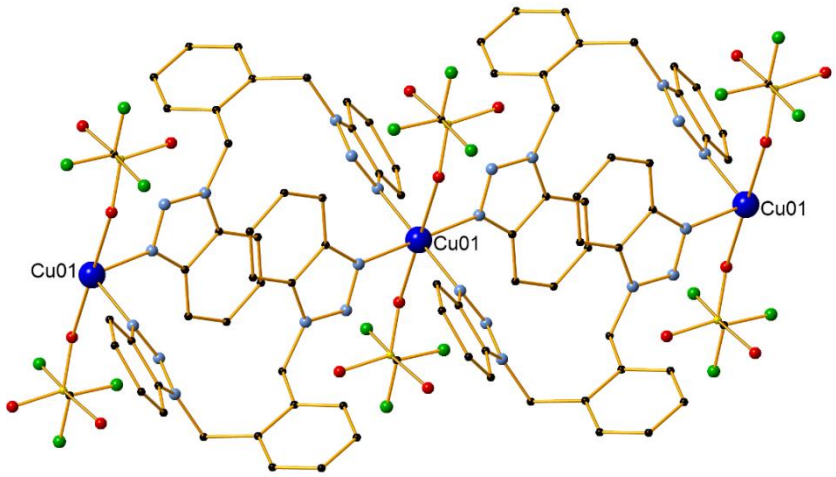

Figure 5. Part of the one-dimensional framework of **8**. H atoms are omitted for clarity. Color code Cu (blue), C (black), N (light blue), O (red), S (yellow), F (light green).

Compound **10** was prepared using L^2 and crystallizes in the monoclinic C2/c space group. The structure is similar to the one of compound **6** as it contains a dicationic dimer, $[Cu_2L_4(H_2O)_2]^{2+}$, as the main core. Four triflate anions are present in the lattice to complete the charge balance for all metal centers. As a result, the structure is zero-dimensional **(**Figure 6) and the dimer is further stabilized through the formation of two strong O-H···O hydrogen bonds, each formed between a water molecule and a triflate anion. The L^2 ligand behaves similarly to L^1 in the case of compound **6**, adopting the same conformation and coordination mode (Table 1, Mode D). Each metal center shows a $\{N_4O\}$ coordination environment through four ligand nitrogen atoms and one oxygen atom from the water molecule, possessing a distorted square pyramidal ($\tau = 0.29$)[78] geometry. The basal plane of this pyramid consists of three nitrogen atoms and one oxygen and shows a mean deviation of 0.149 Å. Compound **11** may be considered as isoskeletal

to **10** as it contains a similar dimeric core; in this case the two coordinating water molecules are replaced by triflate anions (Figure S5, ESI). Due to the similarities, the resulting zero-dimensional structure will not be further described.

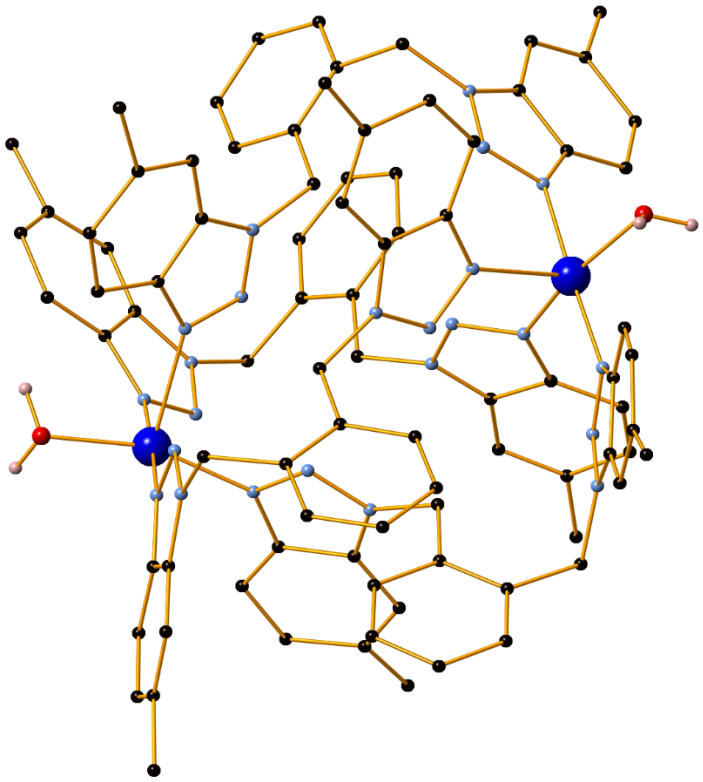

Figure 6. The structure of compound **10**. Lattice solvent molecules, lattice anions and certain H atoms are omitted for clarity. Color code Cu (blue), C (black), N (light blue), O (red), H (light pink).

Table 1. Overview of the coordination characteristics (ligand conformation, coordination geometry of the metal) of the compounds used in this study (S = solvent).

Entry	Compound	Geometry of M(II)	Coordination Mode	Dimensionality
1	**1**	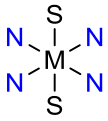	A	1D
2	**2**	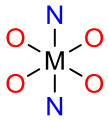	A	2D
3	**3**	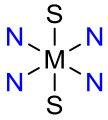	A	1D
4	**4**	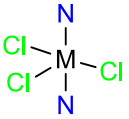	B	0D
5	**5**	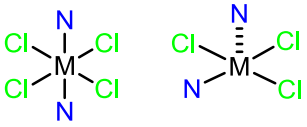	C	2D
6	**6**	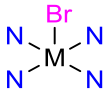	D	0D
7	**7**	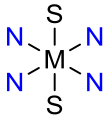	A	1D
8	**8**	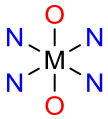	A	1D
9	**9**	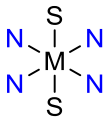	A	1D
10	**10**	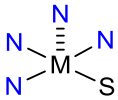	D	0D
11	**11**	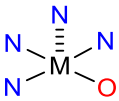	D	0D

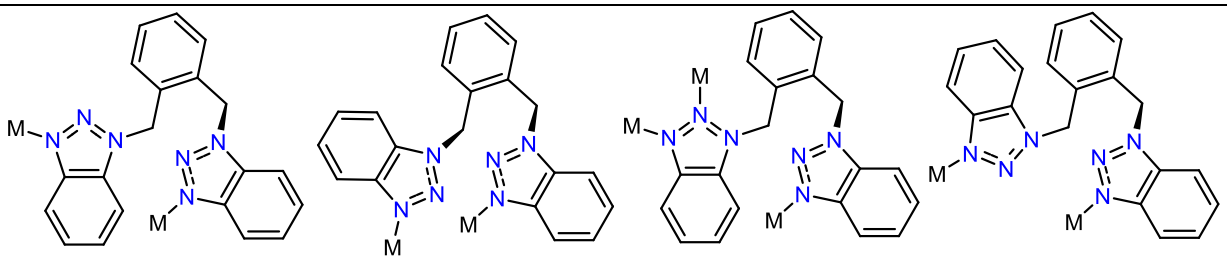

Characterization of compounds 1 - 11. Magnetic measurements for **1** and **2** in the solid state are consistent with octahedral S = ½ Cu(II) centers with $g \sim 2.2$. For **1** there are negligible interactions along the chain (Figure S6, ESI), whilst for **2** we observe a weak short-range ferromagnetic exchange within the dimeric repeat unit of ca. 1 cm^{-1} (Figure S7, ESI). Furthermore, given that the compounds are soluble in most common organic solvents, a range of techniques were used to determine their behavior in solution. ESI-MS (positive-ion mode) in methanolic solution for all Cu(II) complexes (**1**, **2**, **4**-**8**, **10**-**11**) reveals two main peaks which perfectly correspond to the respective $[Cu(L)]^{1+}$ and $[Cu(L)_2]^{1+}$ fragments. Additional peaks are also observed in each spectrum and the main peaks correspond perfectly to metal-ligand-anion fragments; The most common fragments found were $[Cu(L)X]^{1+}$, $[Cu_2(L)X]^{1+}$, $[Cu(L)_2X]^{1+}$, $[Cu(L)_3X]^{1+}$, where X is the anion present in each compound. Similar fragments were obtained for the Zn(II) compounds (**3** and **9**). ESI-MS spectra, along with detailed analysis of the fragments are presented in Figures S8-S18, ESI. These results indicated that the CPs of this study could retain their polymeric structure into the solution. To further clarify this, the same method was applied in a DMF solution of **1**, given that generally DMF molecules can easily coordinate to the metal center. Indeed, the mass spectrum showed identical peaks as above, as well as an additional peak at 575.07 m/z, corresponding perfectly to $[Cu(L^1)(DMF)(ClO_4)]^{1+}$ (Figure S8, ESI).

Additionally, the UV-Vis spectra of **1**, **7**, **8, 10** and **11** in MeOH show a broad peak which is characteristic of *Jahn Teller* effect and consistent for a Cu(II) center with a octahedral $\{N_4O_2\}$ geometry (Figure S19, ESI).

TGA measurements were also conducted to examine the thermal stability of all complexes. In all cases (Figures S20 – S30, ESI), the first mass loss corresponds to the loss of any existing solvent molecules or the counter-anions. The stability of the remaining core is then

retained up to the region of ~300-400 °C, where gradual decomposition takes place. A detailed analysis of the TGA graphs is presented in the Supporting Information.

Catalytic studies. In order to test the possible catalytic activity of **1** – **11**, we studied the application of these catalytic systems in the A^3 coupling of benzaldehyde, pyrrolidine and phenylacetylene (Table 2). During initial experiments with **1** as catalyst we managed to isolate a yellow crystalline material after the end of the reaction, as based on TLC. X-Ray crystallography showed that this material corresponds to the Cu(I) coordination polymer $[Cu^{I}(L^{1})Cl]$ (**1'**), which has already been reported and found to inhibit the catalytic performance of **1**[69] (Table 3, Entry 1). To avoid the conversion issue, we therefore employed **8** in the following optimization procedures.

Furthermore, after screening a variety of solvents for the title reaction, 2-propanol (iPrOH) (an environmentally friendly solvent)[79] was found to provide excellent yields when the reaction mixture was heated to 90^{o}C (Table S3, Entry 6, ESI), while other common organic solvents (such as DMF, acetonitrile, DCM) afforded lower yields. In addition, the reaction was found to be catalyzed by only 0.02 mmol of the catalyst (in 1 mmol reaction scale of benzaldehyde), at 90^{o}C and under air atmosphere (TON = 44.5, TOF = 3.71 hr^{-1}).

Table 2. Overview of the characteristics and catalytic activity of the coordination polymers in this study.

Entry	Compound	Geometry of M(II)	Yield[a, b]
1	**1**	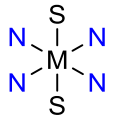	68%
2	**2**	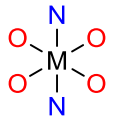	<5%
3	**3**	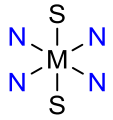	<10%
4	**4**	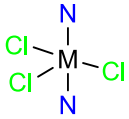	NR[c]
5	**5**	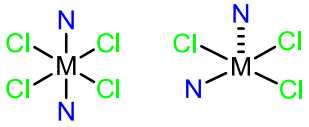	NR[c]
6	**6**	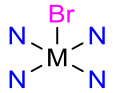	NR[c]
7	**7**	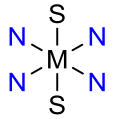	64%
8	**8**	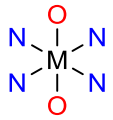	89%(85%)[d]
9	**9**	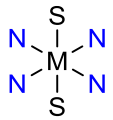	21%
10	**10**	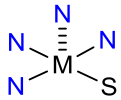	57%
11	**11**	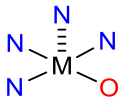	44%

[a] Isolated yields based on aldehyde. [b] Reaction conditions: benzaldehyde (102 μL, 1 mmol), pyrrolidine (90μL, 1.1 mmol), phenylacetylene (132 mL, 1.2 mmol), catalyst (2 mol%), iPrOH (5 ml), T = 90ºC, 12 hr stirring. [c] No reaction. [d] The reaction was performed in presence of 10% TEMPO.

To evaluate the catalytic activity of our compound, several control experiments with common Cu(II) salts were performed for the same A^3 reaction and the results are summarized in Table 3. In all cases, the corresponding Cu(II) salts afforded significantly lower yields,

ranged from 55 to 65%, at higher catalyst loading ca. 10 mol%, based on the benzaldehyde amount (Table 4, entries 1-8). Moreover, the use of Cu(II) salts as catalysts in this A^3 coupling with other *para*-substituted benzaldehydes (such as the 4-chloro-, 4-trifluoromethyl-, 4-methoxy-) instead of benzaldehyde, yielded the corresponding product in low yields (10-15%) showcasing their limited catalytic efficiency. In absence of catalyst no reaction was observed, result that supports the catalytic behavior of the studied multi-component coupling.

Table 3. Evaluation of various Cu salts as catalysts in the multi-component coupling of phenylacetylene, pyrrolidine and benzaldehyde.

Entry	**Catalyst**	[**product**][a] %
1	$CuCl_2$	64
2	$Cu(NO_3)_2 \cdot 2.5H_2O$	65
3	$Cu(ClO_4)_2 \cdot 6H_2O$	60
4	$CuBr_2$	64
5	$CuBF_2 \cdot 6H_2O$	55
6	$Cu(OAc)_2 \cdot H_2O$	58
7	$Cu(OTf)_2 \cdot H_2O$	53
8	$Cu(OTf)_2 \cdot H_2O$[c]	55
9	No catalyst	NR[b]

[a] Reaction conditions: Benzaldehyde (102 μL, 1 mmol), pyrrolidine (90μL, 1.1 mmol), phenylacetylene (132 μL, 1.2 mmol), catalyst (10 mol%), iPrOH (5 ml), heated at 90°C for 12 hr. Isolated yields based on aldehyde. [b] No reaction. [c] Two equivalents of L^1 were added to the reaction mixture.

We then explored the scope of the reaction by employing a variety of aldehydes, amines and alkynes. The results are presented in Scheme 2. Using different aldehydes, pyrrolidine as the amine and phenylacetylene under the above described conditions, a variety of alkyl and aryl substituted propargylamines (**1a**-**1k**) were formed in moderated to high isolated yields. In particular, saturated aliphatic aldehydes react with higher isolated yields (98-100%), compared to the aromatic aldehydes that shows slightly lower reactivity with moderate yields in the range

of 57 to 89%. Consequently, the results of the amine screening (**1l-1u**) indicate that only secondary amines lead to reaction completion, in contrast to primary amines in which no reaction was observed. In general, cyclic aliphatic and aromatic secondary amines afford the corresponding propargylamine products in excellent yields, ranging from 98 to 100%.; acyclic secondary amines were found to be slightly less effective. Finally, the employment of 1-hexyne and 4-trifluoromethylphenylacetylene in the reaction process (**1v-1x**), demonstrated that both alkynes react with the produced imine forming the corresponding propargyl products in good to excellent yields.

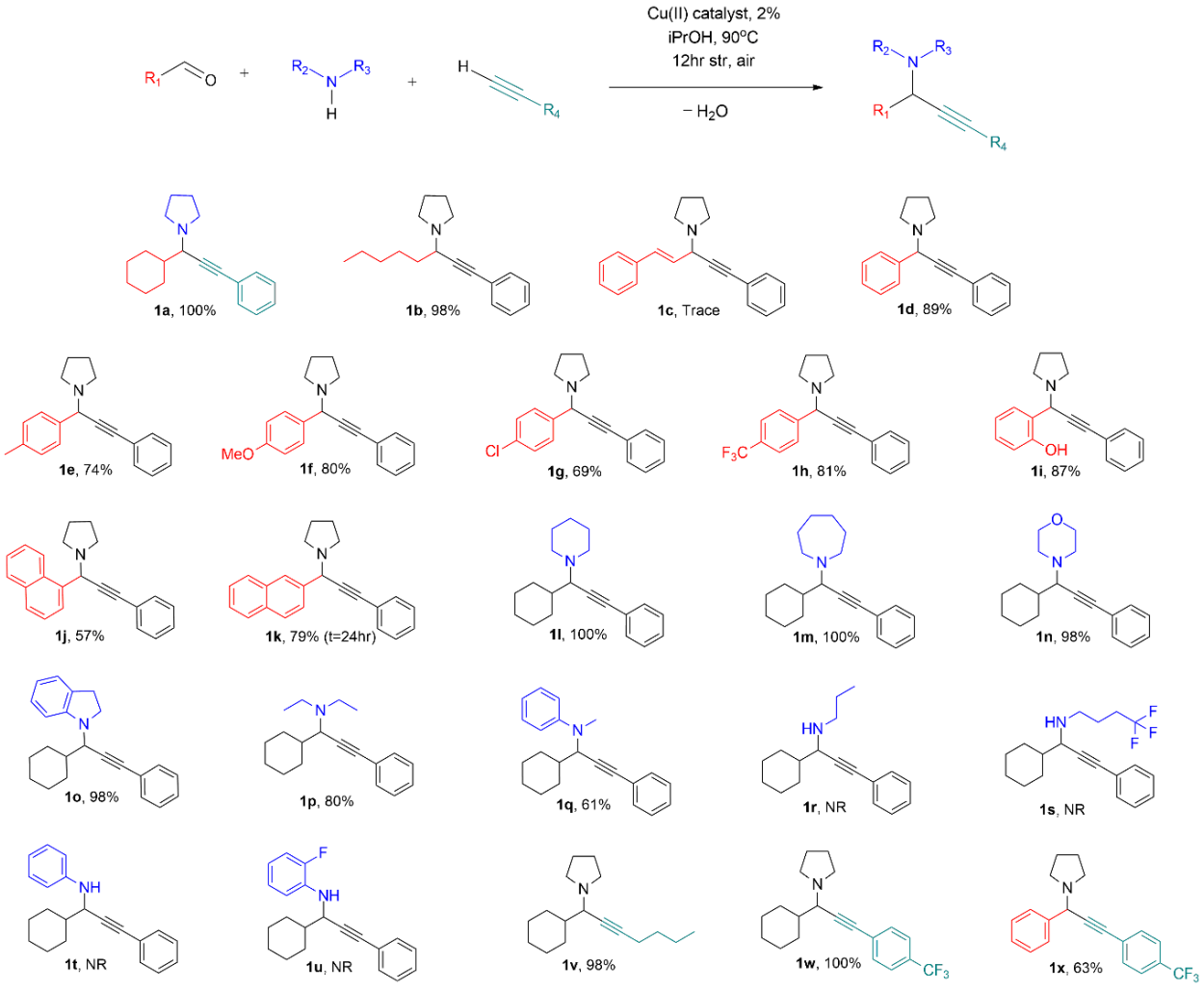

Scheme 2. Catalytic activity of **8** in the A^3 coupling between aldehydes, amines and substituted acetylenes towards propargylamine derivatives synthesis.

Mechanistic aspects. In order to investigate the role of CPs in the reaction and shed light into the reaction mechanism, we focused on synthesizing a variety of Cu(II) coordination polymers with the same ligand by fine tuning their composition; this would enable us to optimize their catalytic performance and see how factors such as the metal geometry or the different anion in the compounds would affect the catalytic activity. Our previous experience and familiarity with the ligand proved critical for this targeted synthesis, and as a result we obtained compounds which possess the desired characteristics (these are further detailed in Tables 1 and 2). **2** was synthesized using $Cu(NO_3)_2 \cdot 2.5H_2O$ and the metal center has a coordination environment of $\{N_2O_5\}$, possessing a pseudo octahedral geometry. The resulting 2D CP, however, only accounted for disappointing yields when tested as a catalyst (Table 2, Entry 2). The employment of halogen copper sources afforded complexes **4**, **5** and **6**, which show considerable differences. The presence of a coordinating anion once again affects the resulting coordination environments ($\{N_2Cl_3\}$, $\{N_2Cl_4\}$, $\{N_4Br\}$) and geometries (trigonal bipyramidal, octahedral), which can be found in further detail in Table 1 (Entries 4, 5, 6). Nevertheless, none of the compounds show any catalytic activity in the tested reaction. Furthermore, by using Cu(II) sources with traditionally non-coordinating anions (as in the case of our initial catalyst, **1**), we were able to isolate compounds **7** and **8**. Both compounds show an identical 1D framework and solution behavior compared to **1** and only the present anion is different. The use of **7** as a catalyst (Table 2, Entry 7) provided results similar to **1**. This indicated that a similar Cu(I) specie is generated, possibly through the conversion of $BF4^-$ to F^- (further supported by the ESI-MS analysis of **7**, in which several peaks containing F^- as the anion were observed) and inhibits the performance of the catalyst. To our delight however, **8** showed very good catalytic activity in the tested reaction, with yields similar to the initial catalyst (Table 2, Entry 8). To investigate its electron donating capabilities, the electrochemistry of **8** was studied by cyclic voltammetry (CV). CV in the cathodic direction over several cycles showed a quasi-

reversible reduction process at -0.423 V vs $Fc^{+/0}$ (i_a/i_c = 1.5) (Figure 7) vs $FeCp_2^{+/0}$ and a non-reversible reduction process[80] at -1.156 V vs $Fc^{+/0}$. The former may be assigned to the $[Cu^{II}]\leftrightarrow[Cu^{I}]$ couple, further supporting the formation of a Cu(I) intermediate during the catalytic reaction. Additional control experiments were then performed to investigate the importance of the redox potential. Given that Zn(II) has lower potential than Cu(II), we employed compounds **3** and **9**; both are 1D Zn(II) CPs with the same framework and have similar thermal and solution behavior. In the case of **3**, the corresponding propargylamine was afforded only at 10% yield (Table 2, Entry 3). Interestingly, compound **9** (Zn(II)), which is isostructural to **8** (Cu(II)), was found to catalyze the title reaction in only 21% yield, as determined by ^{1}H NMR (Table 2, entry 9).

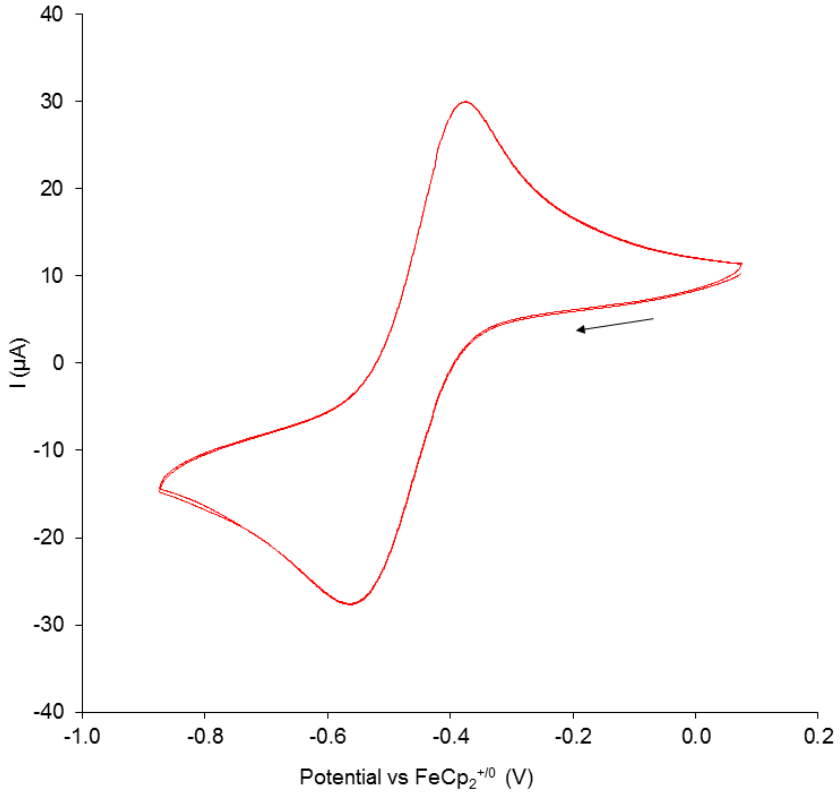

Figure 7. Overlaid CV scans (2 cycles) of **8** in 0.05 M $[^nBu_4N][PF_6]$/DMSO. Scan rate 300 mVs -1 .

The use of the modified benzotriazole derivatives in position 5 (L^2) or positions 5,6 (L^3) yielded the corresponding dimers, **10** and **11**, and not the anticipated 1D CP. The latter were found to moderate catalyze the reaction (Table 2, Entries 10 and 11). In both structures, each Cu(II) center coordinates to 4N atoms (from 4 different ligands) and one O atom, adopting a distorted square planar geometry. However, the UV-Vis spectra show that the Cu(II) centers in **10** and **11** adopt an octahedral geometry (4N+2O) and possibly upon solvation 4 N atoms and 2 O atoms, from four ligands and two MeOH solvated molecules (catalysis takes place in iPrOH), occupy the equatorial and axial positions, respectively. In this way, the adaption of the symmetrical $\{N_4\}$ plane in solution yields the anticipated 1D CP and this transformation may explain the catalytic activity of **10** and **11**. However, the poorer catalytic performance of **10** and **11** in comparison to **8** may be explained by the following factors or a combination of them: A) The aforementioned "in situ" transformation is required for **10** and **11** to behave as catalysts, B) Substitution in position(s) 5(6) of the benzotriazole moieties may attribute a second coordination sphere effect to Cu centers. C) The presence of different axial ligands H_2O (**10**) or Br (**6**) vs OTf (**8**) may disrupt the aforementioned "in situ" transformation or decrease the reactivity of the catalysts.[81,82] Finally, the use of Cu^ICl as the metal source resulted in the synthesis of the catalytically inactive $[Cu^I(L^1)Cl]$ (**1'**) species. It is also worth noting that the addition of 10 mol % of TEMPO did not affect the reaction yield, showcasing the absence of a clear radical process containing the Cu(I)-complex species and supporting the plausible *in-situ* formation of the copper(I)-acetylide intermediate, that is responsible for the catalytic cycle (Scheme S1).

Based on the above observations, the presence of a Cu(II) center in the solution featuring an octahedral geometry with four nitrogen atoms occupying the equatorial positions, is important in order to promote catalytic activity. Furthermore, the choice of the proper anion is critical. The desired catalytically active motif (4N+2O) can be reproduced by the use of non-

coordinating anions. In contrast, the use of other anions results in different coordination geometries and dimensionalities, with zero catalytic activity. These observations are also consistent with the commonly suggested mechanism of the A^3 coupling, which involves the activation of the alkyne by the catalyst (Scheme S1). The planar $\{N_4\}$ geometry of Cu(II) promotes the coordination of the alkyne with concomitant activation of the C–H bond and the formation of the corresponding Cu(I)-acetylide (the acetylenic hydrogen might be abstracted from the hydroxyl anions produced from the iminium ion formation). Consequently, the symmetrical $\{N_4\}$ plane accounts for adequate electron delocalization to ensure the reduction of Cu(II) to Cu(I), which is further promoted by the redox potential of Cu(II). Finally, addition of the Cu(I) acetylide to the *in situ* generated iminium ion yields the corresponding propargylamine derivative and water, and regeneration of the catalyst. The proposed catalytic pathway can be supported, in part, by the recently reported kinetic studies on the effect of alcoholic solvents to Cu(II) Schiff base complexes,[81] and Cu(II)-catalyzed aerobic oxidation of benzylic alcohols in an imidazole containing N_4 ligand framework.[82]

CONCLUSION

In this work, we have introduced a system of 1D Cu(II) CPs that can catalyze the multicomponent reaction of aldehydes, amines and alkynes to produce propargylamine derivatives. In particular, fine-tuning of the catalyst allowed us to generate a 1D CP with excellent catalytic activity, avoiding any issues that would inhibit its performance. The method uses relatively mild conditions and provides results for a broad range of substrates, especially when aliphatic aldehydes and secondary amines are employed. Furthermore, it eliminates the need for expensive metal salts, inert atmosphere or high loadings. We have also attempted to shed more light on the mechanism of the reaction, from an inorganic point of view; through a thorough synthesis and study of targeted CPs, we evaluated how factors like coordination

geometry, anion, ligand tuning affect the catalytic activity. The results are consistent with the suggested mechanism. We envision that this work demonstrates the catalytic potential of the rarely used 1D CPs. As such, our future efforts will be dedicated to a) synthesize variations of **8** with the use of substituted benzotriazole derivatives with electron donating or withdrawing groups, b) use the present library of catalysts to other chemical transformations and c) employ CPs of other metals in the given A^3 coupling reaction.

Supporting Information Available: Crystallographic data, Additional figures of certain structures Magnetic measurements, ESI-MS analysis for **1-11**, UV-Vis spectra, Thermogravimetric analysis for **1-11**, Evaluation of catalytic conditions, Characterization data for A^3-coupling products (^{1}H, ^{13}C NMR and HRMS spectra)

Acknowledgements

We thank the EPSRC UK National Electron Paramagnetic Resonance Service at the University of Manchester for providing magnetic measurements of selected Cu(II) compounds. We thank the EPSRC UK National Crystallography Service at the University of Southampton for the collection of the crystallographic data for compounds **6**-**8** and **10**.[70] I.N.L. and M.K. acknowledge the sponsorship of the Short Term Scientific Mission from COST action CM1201.

References

(1) Batten, S. R.; Champness, N. R.; Chen, X.-M.; Garcia-Martinez, J.; Kitagawa, S.; Öhrström, L.; O'Keeffe, M.; Paik Suh, M.; Reedijk, J. Terminology of Metal–organic Frameworks and Coordination Polymers (IUPAC Recommendations 2013). *Pure Appl. Chem.* **2013**, *85*, 1715–1724 DOI: 10.1351/PAC-REC-12-11-20.

(2) Yan, Y.; Juríček, M.; Coudert, F.-X.; Vermeulen, N. A.; Grunder, S.; Dailly, A.; Lewis, W.; Blake, A. J.; Stoddart, J. F.; Schröder, M. Non-Interpenetrated Metal–Organic Frameworks Based on Copper(II) Paddlewheel and Oligoparaxylene-Isophthalate Linkers: Synthesis, Structure, and Gas Adsorption. *J. Am. Chem. Soc.* **2016**, *138*, 3371–3381 DOI: 10.1021/jacs.5b12312.

(3) Rojas, S.; Carmona, F. J.; Maldonado, C. R.; Horcajada, P.; Hidalgo, T.; Serre, C.; Navarro, J. A. R.; Barea, E. Nanoscaled Zinc Pyrazolate Metal–Organic Frameworks as Drug-Delivery Systems. *Inorg. Chem.* **2016**, *55*, 2650–2663 DOI: 10.1021/acs.inorgchem.6b00045.

(4) Horcajada, P.; Chalati, T.; Serre, C.; Gillet, B.; Sebrie, C.; Baati, T.; Eubank, J. F.; Heurtaux, D.; Clayette, P.; Kreuz, C.; Chang, J.-S.; Hwang, Y. K.; Marsaud, V.; Bories, P.-N.; Cynober, L.; Gil, S.; Férey, G.; Couvreur, P.; Gref, R. Porous Metal–organic-Framework Nanoscale Carriers as a Potential Platform for Drug Delivery and Imaging. *Nat. Mater.* **2010**, *9*, 172–178 DOI: 10.1038/nmat2608.

(5) Cui, Y.; Chen, B.; Qian, G. Lanthanide Metal-Organic Frameworks for Luminescent Sensing and Light-Emitting Applications. *Coord. Chem. Rev.* **2014**, *273–274*, 76–86 DOI: 10.1016/j.ccr.2013.10.023.

(6) Zeng, M. H.; Yin, Z.; Tan, Y. X.; Zhang, W. X.; He, Y. P.; Kurmoo, M. Nanoporous cobalt(II) MOF Exhibiting Four Magnetic Ground States and Changes in Gas Sorption upon Post-Synthetic Modification. *J. Am. Chem. Soc.* **2014**, *136*, 4680–4688 DOI:

10.1021/ja500191r.

(7) Liu, D.; Lu, K.; Poon, C.; Lin, W. Metal-Organic Frameworks as Sensory Materials and Imaging Agents. *Inorg. Chem.* **2014**, *53*, 1916–1924 DOI: 10.1021/ic402194c.

(8) Thacker, N. C.; Lin, Z.; Zhang, T.; Gilhula, J. C.; Abney, C. W.; Lin, W. Robust and Porous β-Diketiminate-Functionalized Metal–Organic Frameworks for Earth-Abundant-Metal-Catalyzed C–H Amination and Hydrogenation. *J. Am. Chem. Soc.* **2016**, *138*, 3501–3509 DOI: 10.1021/jacs.5b13394.

(9) Kaye, S. S.; Dailly, A.; Yaghi, O. M.; Long, J. R. Impact of Preparation and Handling on the Hydrogen Storage Properties of Zn4O(1,4-benzenedicarboxylate)3 (MOF-5). *J. Am. Chem. Soc.Chem. Soc.* **2007**, *129*, 14176–14177 DOI: 10.1021/ja076877g.

(10) Maji, T. K.; Matsuda, R.; Kitagawa, S. A Flexible Interpenetrating Coordination Framework with a Bimodal Porous Functionality. *Nat. Mater.* **2007**, *6*, 142–148 DOI: 10.1038/nmat1827.

(11) Yang, J.-X.; Qin, Y.-Y.; Cheng, J.-K.; Zhang, X.; Yao, Y.-G. Construction of a Series of Zn(II) Compounds with Different Entangle Motifs by Varying Flexible Aliphatic Dicarboxylic Acids. *Cryst. Growth Des.* **2015**, *15*, 2223–2234 DOI: 10.1021/cg501879w.

(12) Leong, W. L.; Vittal, J. J. One-Dimensional Coordination Polymers: Complexity and Diversity in Structures, Properties, and Applications. *Chem. Rev.* **2011**, *111*, 688–764 DOI: 10.1021/cr100160e.

(13) Sutradhar, M.; Guedes da Silva, M. F. C.; Nesterov, D. S.; Jezierska, J.; Pombeiro, A. J. L. 1D Coordination Polymer with Octahedral and Square-Planar nickel(II) Centers. *Inorg. Chem. Commun.* **2013**, *29*, 82–84 DOI: 10.1016/j.inoche.2012.12.008.

(14) Mendes, R. F.; Silva, P.; Antunes, M. M.; Valente, A. A.; Almeida Paz, F. A. Sustainable Synthesis of a Catalytic Active One-Dimensional Lanthanide-Organic Coordination

Polymer. *Chem. Commun.* **2015**, *51*, 10807–10810 DOI: 10.1039/c5cc01888a.

(15) Dias, S. S. P.; Kirillova, M. V; André, V.; Kłak, J.; Kirillov, A. M. New Tetracopper(II) Cubane Cores Driven by a Diamino Alcohol: Self-Assembly Synthesis, Structural and Topological Features, and Magnetic and Catalytic Oxidation Properties. *Inorg. Chem.* **2015**, *54*, 5204–5212 DOI: 10.1021/acs.inorgchem.5b00048.

(16) Sotnik, S. A.; Polunin, R. A.; Kiskin, M. A.; Kirillov, A. M.; Dorofeeva, V. N.; Gavrilenko, K. S.; Eremenko, I. L.; Novotortsev, V. M.; Kolotilov, S. V. Heterometallic Coordination Polymers Assembled from Trigonal Trinuclear Fe 2 Ni-Pivalate Blocks and Polypyridine Spacers: Topological Diversity, Sorption, and Catalytic Properties. *Inorg. Chem.* **2015**, *54*, 5169–5181 DOI: 10.1021/ic503061z.

(17) Dias, S. S. P.; Kirillova, M. V.; André, V.; Kłak, J.; Kirillov, A. M. New tricopper(II) Cores Self-Assembled from Aminoalcohol Biobuffers and Homophthalic Acid: Synthesis, Structural and Topological Features, Magnetic Properties and Mild Catalytic Oxidation of Cyclic and Linear C 5 –C 8 Al. *Inorg. Chem. Front.* **2015**, *2*, 525–537 DOI: 10.1039/C4QI00220B.

(18) Kirillov, A. M.; Karabach, Y. Y.; Kirillova, M. V; Haukka, M.; Pombeiro, A. J. L. Topologically Unique 2D Heterometallic Cu II/Mg Coordination Polymer: Synthesis, Structural Features, and Catalytic Use in Alkane Hydrocarboxylation. *Cryst. Growth Des.* **2012**, *12*, 1069–1074 DOI: 10.1021/cg201459k.

(19) Peshkov, V. A.; Pereshivko, O. P.; Van Der Eycken, E. V. A Walk around the A 3 - Coupling. *Chem. Soc. Rev.* **2012**, *41*, 3790–3807 DOI: 10.1039/c2cs15356d.

(20) Fan, W.; Yuan, W.; Ma, S. Unexpected E-Stereoselective Reductive A(3)-Coupling Reaction of Terminal Alkynes with Aldehydes and Amines. *Nat. Commun.* **2014**, *5*, 1472–1483 DOI: 10.1038/ncomms4884.

(21) Kaur, S.; Kumar, M.; Bhalla, V. Aggregates of Perylene Bisimide Stabilized

Superparamagnetic Fe3O4 Nanoparticles: An Efficient Catalyst for the Preparation of Propargylamines and Quinolines via C-H Activation. *Chem. Commun.* **2015**, *51*, 16327–16330 DOI: 10.1039/C5CC05752C.

(22) Paioti, P. H. S.; Abboud, K. A.; Aponick, A. Catalytic Enantioselective Synthesis of Amino Skipped Diynes. *J. Am. Chem. Soc.* **2016**, *138*, 2150–2153 DOI: 10.1021/jacs.5b13387.

(23) De, D.; Pal, T. K.; Neogi, S.; Senthilkumar; Das, D.; Gupta, S. Sen; Bharadwaj, P. K. A Versatile CuII Metal-Organic Framework Exhibiting High Gas Storage Capacity with Selectivity for CO2: Conversion of CO2 to Cyclic Carbonate and Other Catalytic Abilities. *Chem. - A Eur. J.* **2016**, *22*, 3387–3396.

(24) Zhao, H.; He, W.; Wei, L.; Cai, M. A Highly Efficient Heterogeneous Copper-Catalyzed Three-Component Coupling of Tetrahydroisoquinolines, Aldehydes and 1-Alkynes. *Catal. Sci. Technol.* **2016**, *6*, 1488–1495.

(25) Varyani, M.; Khatri, P. K.; Jain, S. L. Amino Acid Ionic Liquid Bound Copper Schiff Base Catalyzed Highly Efficient Three Component A3-Coupling Reaction. *Catal. Commun.* **2016**, *77*, 113–117.

(26) Chen, H.-B.; Zhao, Y.; Liao, Y. Aldehyde-Alkyne-Amine (A3) Coupling Catalyzed by a Highly Efficient Dicopper Complex. *RSC Adv.* **2015**, *5*, 37737–37741.

(27) Sugiishi, T.; Kimura, A.; Nakamura, H. Copper(I)-Catalyzed Substitution Reactions of Propargylic Amines: Importance of C(sp)-C(sp3) Bond Cleavage in Generation of Iminium Intermediates. *J. Am. Chem. Soc.* **2010**, *132*, 5332–5333.

(28) Chauhan, D. P.; Varma, S. J.; Vijeta, A.; Banerjee, P.; Talukdar, P. A 1,3-Amino Group Migration Route to Form Acrylamidines. *Chem Commun* **2014**, *50*, 323–325 DOI: 10.1039/c3cc47182a.

(29) Arcadi, A.; Cacchi, S.; Cascia, L.; Fabrizi, G.; Marinelli, F. Preparation of 2,5-

Disubstituted Oxazoles from N-Propargylamides. *Org. Lett.* **2001**, *3*, 2501–2504 DOI: 10.1021/ol016133m.

(30) Nilsson, B. M.; Hacksell, U. Base-Catalyzed Cyclization of *N* -Propargylamides to Oxazoles. *J. Heterocycl. Chem.* **1989**, *26*, 269–275 DOI: 10.1002/jhet.5570260201.

(31) Yamamoto, Y.; Hayashi, H.; Saigoku, T.; Nishiyama, H. Domino Coupling Relay Approach to Polycyclic Pyrrole-2-Carboxylates. *J. Am. Chem. Soc.* **2005**, *127*, 10804–10805.

(32) Harvey, D. F.; Sigano, D. M. Synthesis of Cyclopropylpyrrolidines via Reaction of *N* -Allyl- *N* -Propargylamides with a Molybdenum Carbene Complex. Effect of Substituents and Reaction Conditions. *J. Org. Chem.* **1996**, *61*, 2268–2272 DOI: 10.1021/jo9519930.

(33) Fleming, J. J.; Du Bois, J. A Synthesis of (+)-Saxitoxin. *J. Am. Chem. Soc.* **2006**, *128*, 3926–3927 DOI: 10.1021/ja0608545.

(34) Trost, B. M.; Chung, C. K.; Pinkerton, A. B. Stereocontrolled Total Synthesis of (+)-Streptazolin by a Palladium-Catalyzed Reductive Diyne Cyclization. *Angew. Chemie Int. Ed.* **2004**, *43* (33), 4327–4329 DOI: 10.1002/anie.200460058.

(35) Zhang, X.; Corma, A. Supported gold(III) Catalysts for Highly Efficient Three-Component Coupling Reactions. *Angew. Chemie - Int. Ed.* **2008**, *47*, 4358–4361.

(36) Karimi, B.; Gholinejad, M.; Khorasani, M. Highly Efficient Three-Component Coupling Reaction Catalyzed by Gold Nanoparticles Supported on Periodic Mesoporous Organosilica with Ionic Liquid Framework. *Chem. Commun.* **2012**, *48*, 8961–8963.

(37) Wei, C.; Li, C.-J. A Highly Efficient Three-Component Coupling of Aldehyde, Alkyne, and Amines via C-H Activation Catalyzed by Gold in Water. *J. Am. Chem. Soc.* **2003**, *125*, 9584–9585.

(38) Lo, V. K.-Y.; Zhou, C.-Y.; Wong, M.-K.; Che, C.-M. Silver(I)-Mediated Highly

Enantioselective Synthesis of Axially Chiral Allenes under Thermal and Microwave-Assisted Conditions. *Chem. Commun.* **2010**, *46*, 213–215 DOI: 10.1039/b914516h.

(39) Wei, C.; Li, Z.; Li, C.-J. The First Silver-Catalyzed Three-Component Coupling of Aldehyde, Alkyne, and Amine. *Org. Lett.* **2003**, *5*, 4473–4475.

(40) Zhao, Y.; Zhou, X.; Okamura, T.-A.; Chen, M.; Lu, Y.; Sun, W.-Y.; Yu, J.-Q. Silver Supramolecule Catalyzed Multicomponent Reactions under Mild Conditions. *Dalton Trans.* **2012**, *41*, 5889–5896.

(41) Salam, N.; Sinha, A.; Roy, A. S.; Mondal, P.; Jana, N. R.; Islam, S. M. Synthesis of Silver-Graphene Nanocomposite and Its Catalytic Application for the One-Pot Three-Component Coupling Reaction and One-Pot Synthesis of 1,4-Disubstituted 1,2,3-Triazoles in Water. *RSC Adv.* **2014**, *4*, 10001–10012.

(42) Sharma, N.; Sharma, U. K.; Mishra, N. M.; Van Der Eycken, E. V. Copper-Catalyzed Diversity-Oriented Three- and Five- Component Synthesis of Mono- and Dipropargylic Amines via Coupling of Alkynes, Alpha-Amino Esters and Aldehydes. *Adv. Synth. Catal.* **2014**, *356*, 1029–1037.

(43) Zhao, C.; Seidel, D. Enantioselective A3 Reactions of Secondary Amines with a Cu(I)/Acid-Thiourea Catalyst Combination. *J. Am. Chem. Soc.* **2015**, *137*, 4650–4653.

(44) Shi, L.; Tu, Y.-Q.; Wang, M.; Zhang, F.-M.; Fan, C.-A. Microwave-Promoted Three-Component Coupling of Aldehyde, Alkyne, and Amine via C-H Activation Catalyzed by Copper in Water. *Org. Lett.* **2004**, *6*, 1001–1003.

(45) Trang, T. T. T.; Ermolat'ev, D. S.; Van der Eycken, E. V. Facile and Diverse Microwave-Assisted Synthesis of Secondary Propargylamines in Water Using CuCl/CuCl 2. *RSC Adv.* **2015**, *5*, 28921–28924 DOI: 10.1039/C4RA16005C.

(46) Zhang, Y.; Li, P.; Wang, M.; Wang, L. Indium-Catalyzed Highly Efficient Three-Component Coupling of Aldehyde , Alkyne , and Amine via C - H Bond Activation In

This Paper , Indium (III) Chloride Was Found to Be a Highly Effective Catalyst for the Three-Component Coupling Reactions of Aldehyd. *J. Org. Chem.* **2009**, *74*, 4364–4367.

(47) Rubio-Pérez, L.; Iglesias, M.; Munárriz, J.; Polo, V.; Pérez-Torrente, J. J.; Oro, L. A. Efficient Rhodium-Catalyzed Multicomponent Reaction for the Synthesis of Novel Propargylamines. *Chem. - A Eur. J.* **2015**, *21*, 17701–17707 DOI: 10.1002/chem.201502993.

(48) Choudary, B. M.; Sridhar, C.; Kantam, M. L.; Sreedhar, B. Hydroxyapatite Supported Copper Catalyst for Effective Three-Component Coupling. *Tetrahedron Lett.* **2004**, *45*, 7319–7321.

(49) Meyet, C. E.; Pierce, C. J.; Larsen, C. H. A Single Cu (II) Catalyst for the Three-Component Coupling of Diverse Nitrogen Sources with Aldehydes and Alkynes. *Org. Lett.* **2012**, *14*, 964–967.

(50) Pierce, C. J.; Larsen, C. H. Copper(II) Catalysis Provides Cyclohexanone-Derived Propargylamines Free of Solvent or Excess Starting Materials: Sole by-Product Is Water. *Green Chem.* **2012**, *14*, 2672–2676.

(51) Li, P.; Zhang, Y.; Wang, L. Iron-Catalyzed Ligand-Free Three-Component Coupling Reactions of Aldehydes, Terminal Alkynes, and Amines. *Chem. - A Eur. J.* **2009**, *15*, 2045–2049.

(52) Chen, W.-W.; Nguyen, R. V; Li, C.-J. Iron-Catalyzed Three-Component Coupling of Aldehyde, Alkyne, and Amine under Neat Conditions in Air. *Tetrahedron Lett.* **2009**, *50*, 2895–2898.

(53) Huo, X.; Liu, J.; Wang, B.; Zhang, H.; Yang, Z.; She, X.; Xi, P. A One-Step Method to Produce Graphene-Fe3O4 Composites and Their Excellent Catalytic Activities for Three-Component Coupling of Aldehyde, Alkyne and Amine. *J. Mater. Chem. A* **2013**, *1*, 651–656.

(54) Samai, S.; Nandi, G. C.; Singh. An Efficient and Facile One-Pot Synthesis of Propargylamines by Three-Component Coupling of Aldehydes, Amines, and Alkynes via C-H Activation Catalyzed by NiCl2. *Tetrahedron Lett.* **2010**, *51*, 5555–5558.

(55) Ramu, E.; Varala, R.; Sreelatha, N.; Adapa, S. R. Zn(OAc)2·2H2O: A Versatile Catalyst for the One-Pot Synthesis of Propargylamines. *Tetrahedron Lett.* **2007**, *48*, 7184–7190 DOI: 10.1016/j.tetlet.2007.07.196.

(56) Katritzky, A. R.; Rogovoy, B. V. Benzotriazole: An Ideal Synthetic Auxiliary. *Chem. Eur. J.* **2003**, *9*, 4586–4593 DOI: 10.1002/chem.200304990.

(57) Katritzky, A. R.; Rachwal, S. Synthesis of Heterocycles Mediated by Benzotriazole. 1. Monocyclic Systems. *Chem. Rev.* **2010**, *110*, 1564–1610 DOI: 10.1021/cr900204u.

(58) Aromí, G.; Barrios, L. A.; Roubeau, O.; Gamez, P. Triazoles and Tetrazoles: Prime Ligands to Generate Remarkable Coordination Materials. *Coord. Chem. Rev.* **2011**, *255*, 485–546 DOI: 10.1016/j.ccr.2010.10.038.

(59) Børsting, P.; Steel, P. J. Synthesis and X-Ray Crystal Structures of Cobalt and Copper Complexes of 1,3-Bis(benzotriazolyl)propanes. *Eur. J. Inorg. Chem.* **2004**, 376–380 DOI: 10.1002/ejic.200300271.

(60) Richardson, C.; Steel, P. J. Benzotriazole as a Structural Component in Chelating and Bridging Heterocyclic Ligands; Ruthenium, Palladium, Copper and Silver Complexes. *Dalton Trans.* **2003**, *34*, 992–1000 DOI: 10.1039/b206990c.

(61) Schmieder, P.; Denysenko, D.; Grzywa, M.; Magdysyuk, O.; Volkmer, D. A Structurally Flexible Triazolate-Based Metal–organic Framework Featuring Coordinatively Unsaturated Copper(I) Sites. *Dalton Trans.* **2016**, *45*, 13853–13862 DOI: 10.1039/C6DT02672A.

(62) Tangoulis, V.; Raptopoulou, C. P.; Psycharis, V.; Terzis, A.; Skorda, K.; Perlepes, S. P.; Cador, O.; Kahn, O.; Bakalbassis, E. G. Ferromagnetism in an Extended Three-

Dimensional, Diamond-like copper(II) Network: A New copper(II)/1-Hydroxybenzotriazolato Complex Exhibiting Soft-Magnet Properties and Two Transitions at 6.4 and 4.4 K. *Inorg. Chem.* **2000**, *39*, 2522–2529 DOI: 10.1021/ic991149i.

(63) Wang, X.-L.; Qin, C.; Wu, S.-X.; Shao, K.-Z.; Lan, Y.-Q.; Wang, S.; Zhu, D.-X.; Su, Z.-M.; Wang, E.-B. Bottom-up Synthesis of Porous Coordination Frameworks: Apical Substitution of a Pentanuclear Tetrahedral Precursor. *Angew. Chem. Int. Ed.* **2009**, *48*, 5291–5295 DOI: 10.1002/anie.200902274.

(64) Biswas, S.; Tonigold, M.; Speldrich, M.; Kögerler, P.; Volkmer, D. Nonanuclear Coordination Compounds Featuring {M 9 L 12 } 6+ Cores (M = Ni II , Co II , or Zn II ; L = 1,2,3-Benzotriazolate). *Eur. J. Inorg. Chem.* **2009**, 3094–3101 DOI: 10.1002/ejic.200900156.

(65) Collison, D.; McInnes, E. J. L.; Brechin, E. K. Tetrahedra, Super-Tetrahedra, Bipyramids, Boxes and More: Polymetallic Clusters of Benzotriazole. *Eur. J. Inorg. Chem.* **2006**, 2725–2733 DOI: 10.1002/ejic.200600206.

(66) Loukopoulos, E.; Griffiths, K.; Akien, G. R.; Kourkoumelis, N.; Abdul-Sada, A.; Kostakis, G. E. Dinuclear Lanthanide (III) Coordination Polymers in a Domino Reaction. *Inorganics* **2015**, *3*, 448–466.

(67) Kostakis, G. E.; Xydias, P.; Nordlander, E.; Plakatouras, J. C. The First Structural Determination of a Copper (II) Complex Containing the Ligand [1-(4-((1H-benzo[d][1,2,3]triazol-2(3H)-Yl)methyl)benzyl)-1H-benzo[d][1,2,3]triazole]. *Inorg. Chim. Acta* **2012**, *383*, 327–331 DOI: 10.1016/j.ica.2011.10.063.

(68) Loukopoulos, E.; Chilton, N.; Abdul-Sada, A.; Kostakis, G. E. Exploring the Coordination Capabilities of a Family of Flexible Benzotriazole-Based Ligands Using Cobalt (II) Sources. *Cryst. Growth Des.* **2017**, *under revi*.

(69) Kallitsakis, M.; Loukopoulos, E.; Abdul-Sada, A.; Tizzard, G. J.; Coles, S. J.; Kostakis, G. E.; Lykakis, I. N. A Copper-Benzotriazole-Based Coordination Polymer Catalyzes the Efficient One-Pot Synthesis of (*N′* -Substituted)-Hydrazo-4-Aryl-1,4-Dihydropyridines from Azines. *Adv. Synth. Catal.* **2017**, *359*, 138–145 DOI: 10.1002/adsc.201601072.

(70) Coles, S. J.; Gale, P. A. Changing and Challenging Times for Service Crystallography. *Chem. Sci.* **2012**, *3*, 683–689 DOI: 10.1039/c2sc00955b.

(71) Dolomanov, O. V; Blake, A. J.; Champness, N. R.; Schröder, M. OLEX: New Software for Visualization and Analysis of Extended Crystal Structures. *J. Appl. Crystallogr.* **2003**, *36*, 1283–1284.

(72) Sheldrick, G. M. SHELXT – Integrated Space-Group and Crystal-Structure Determination. *Acta Crystallogr. Sect. A Found. Adv.* **2015**, *71*, 3–8 DOI: 10.1107/S2053273314026370.

(73) Sheldrick, G. M. SHELXS97, Program for the Solution of Crystal Structures. *Acta Crystallogr. Sect. A* **2008**, *64*, 112–122.

(74) Farrugia, L. J. Suite for Small-Molecule Single-Crystal Crystallography. *J. Appl. Crystallogr.* **1999**, *32*, 837–838 DOI: 10.1107/S0021889899006020.

(75) Spek, A. L. Single-Crystal Structure Validation with the Program PLATON. *J. Appl. Crystallogr.* **2003**, *36*, 7–13 DOI: 10.1107/S0021889802022112.

(76) Macrae, C. F.; Edgington, P. R.; McCabe, P.; Pidcock, E.; Shields, G. P.; Taylor, R.; Towler, M.; Van De Streek, J. Mercury: Visualization and Analysis of Crystal Structures. *J. Appl. Crystallogr.* **2006**, *39*, 453–457 DOI: 10.1107/S002188980600731X.

(77) Allen, F. H. The Cambridge Structural Database: A Quarter of a Million Crystal Structures and Rising. *Acta Crystallogr. Sect. B-Structural Sci.* **2002**, *58*, 380–388 DOI:

10.1107/s0108768102003890.

(78) Addison, A. W.; Rao, T. N.; Reedijk, J.; van Rijn, J.; Verschoor, G. C. Synthesis, Structure, and Spectroscopic Properties of copper(II) Compounds Containing Nitrogen?sulphur Donor Ligands; the Crystal and Molecular Structure of aqua[1,7-bis(N-Methylbenzimidazol-2?-Yl)-2,6-dithiaheptane]copper(II) Perchlorate. *J. Chem. Soc. Dalton Trans.* **1984**, 1349 DOI: 10.1039/dt9840001349.

(79) Prat, D.; Hayler, J.; Wells, A. A Survey of Solvent Selection Guides. *Green Chem.* **2014**, *16* , 4546–4551 DOI: 10.1039/C4GC01149J.

(80) This Process Was Found to Interfere with the First Process upon Scanning in the Anodic Direction, Possibly due to an Electrochemically Produced Species.

(81) Zhang, W.; Saraei, N.; Nie, H.; Vaughn, J. R.; Jones, A. S.; Mashuta, M. S.; Buchanan, R. M.; Grapperhaus, C. A. Reversible Methanol Addition to Copper Schiff Base Complexes: A Kinetic, Structural and Spectroscopic Study of Reactions at Azomethine C□N Bonds. *Dalton Trans.* **2016**, *45*, 15791–15799 DOI: 10.1039/C6DT01955B.

(82) Jain, R.; Gibson, T. J.; Mashuta, M. S.; Buchanan, R. M.; Grapperhaus, C. A. Copper Catalysed Aerobic Oxidation of Benzylic Alcohols in an Imidazole Containing N 4 Ligand Framework. *Dalton Trans.* **2016**, *45*, 18356–18364 DOI: 10.1039/C6DT03395D.

For Table of Contents Only

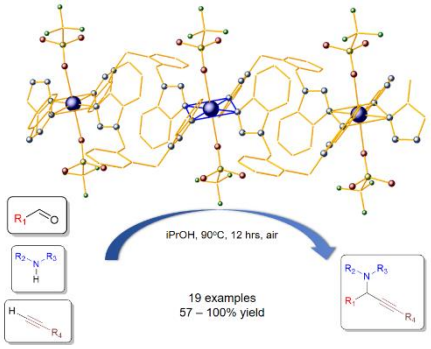

A series of Cu(II) benzotriazole based coordination polymers is introduced as excellent homogeneous catalysts for the A^3 coupling synthesis of propargyl amine derivatives.